JCE
Journal of Civil Engineering
ISSN 2086 - 1206 E-ISSN 2579 - 9029

Modeling Reinforced Concrete Column with GRFP Transverse Reinforcement

Haura Adena[a], Harun Alrasyid[a*], Wahyuniarsih Sutrisno[a], Bambang Piscesa[a]

Correspondence

[a]Civil Engineering Department, Sepuluh Nopember Institute of Technology (ITS), Surabaya, Indonesia.

Corresponding author email address:harun@its.ac.id

Submitted : 18 November 2024
Revised : 31 January 2025
Accepted : 19 February 2025

Abstract

The utilization of GFRP (Glass Fiber Reinforced Polymer) in reinforced concrete structures is gaining attention due to its high strength and low corrosion. The application of GRFP rebar as longitudinal and tranverse reinforced columns has been studied through experimental testing. However it is important to understand the deformation responses and to predict the behavior of concrete columns with GRFP Rebar. This objective requires suitable and effective tools. This study presents Finite Element Analysis of Concrete Column reinforced with GRFP Rebar using 3DNLFEA. The result showed that The analysis result exhibited that the prediction of model behavior corresponds well with the experimental results.

Keywords

Reinforced concrete column, GFRP rebar, seismic performance, 3DNLFEA

INTRODUCTION

Reinforced concrete columns are among the most commonly used structural elements in building construction. Most reinforced concrete columns in buildings still use steel reinforcement to enhance structural strength. However, the utilization of steel rebar in concrete columns can pose several issues, such as corrosion and excessive weight. Therefore, alternative construction materials are used to address these problems.

In recent years, Fiber Reinforced Polymer (FRP) reinforcement has been widely used as a substitute for steel reinforcement. FRP materials have emerged as an alternative reinforcement for concrete structures. FRP can be made from three composite materials: Carbon, Glass, and Aramid [1]. Among these three composite materials, GFRP is relatively cheaper [2]. GFRP is a polymer matrix composite material that uses resin and glass fibers. The use of GFRP rebar as an alternative to steel rebar in concrete offers many advantages over steel reinforcement, such as higher tensile strength and high corrosion resistance, even in harsh chemical environments [3]

The GFRP reinforcement can lead to sudden and usually explosive damage. However, this failure can be avoided by meeting the required reinforcement ratio, potentially resulting in more progressive and less dangerous failure [4] [5]. FRP bars exhibit linear-elastic behavior up to failure, along with a relatively low modulus of elasticity [6], raising concerns about the efficiency of FRP structures in seismic zones.

Research on FRP-reinforced columns subjected to lateral loading by [5], [7], [8], and [6] showed stable responses and high drift ratios at failure with acceptable energy dissipation levels, confirming the effectiveness of GFRP confinement as transverse reinforcement.

All research on behaviours using GRFP rebar as longitudinal and transverse reinforcement in concrete columns has been conducted using experimental studies. However, due to limited funding and availability of testing facilities, further research on behavior-reinforced concrete columns using GRFP rebar on longitudinal and transverse reinforcement can be performed using the finite element method. The study of concrete columns using GRFP rebar on finite element method was rare performed. This paper will discuss the modelling of reinforced concrete columns using longitudinal and transverse rebar subjected to a loading combination between constant axial load and pushover displacement load. The specimens used as reference is G-1.3-10-100 from the research conducted by [10].

RESEARCH SIGNIFICANCE

This research presents the prediction behaviour of reinforced concrete column using GRFP rebar as longitudinal dan transverse reinforcement using finite element method. The specimen is single curvature columns subjected under combination of constant axial load and monotonic pushover load. The analysis is performed on in-house 3D-NLFEA finite element package.

METHODOLOGY

The research methodology presented in this paper consisted of four stages of preparation: A) Specimen Geometry, B) Boundary condition, C) Material properties and constitutive material, and D) The three-dimensional finite-element method. The 3D-NLFEA finite element package developed by [10] [11]was used. The package uses SALOME as a pre-processor and PARAVIEW as a post-processor. The methodology is described in the following sections

A. SPECIMEN GEOMETRY

The column specimen to be created consists of longitudinal reinforcement, transverse reinforcement, concrete cover, concrete core, and column base. The specimen used is G-1.3-10-100 from the research conducted by [10]. The letter G indicates that the GRFP bar is used for longitudinal and transversal reinforcement for concrete columns. The first number, 1.3, showed the percentage amount the longitudinal reinforcement ratio. The second number, 10, stands for the level of axial load ratio. The last number, 100, exhibited the spacing of transverse reinforcement in mm. The column dimension is a square of 350x350mm^2 , and 1650mm in height. The dimensions of the bottom concrete block are 1400x 1400 x600 mm. Specimen geometry details are shown in Figure 1.

The column was longitudinally reinforced with No. 16 GFRP bars, each with a 15.9 mm diameter, and transversally reinforced with No. 10 stirrups, each with a 9.5 mm diameter. The details of the reinforcing bars are shown in Table 1.

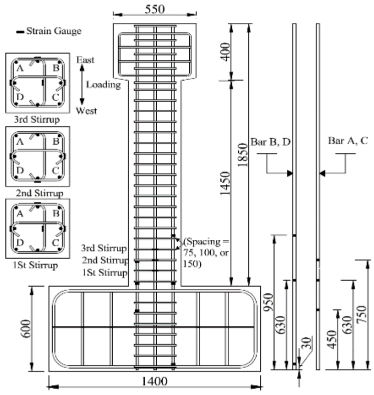

Figure 1. Detail specimen geometry

..

Table 1. Mechanical Properties of GRFP Reinforcing Bars

Bar Type	Bar diameter (mm)	Bar area (mm^2)	Modulus of elasticity (GPa)	Tensile strength (MPa)	Ultimate strain (%)
No. 16	15.9	198	62 ± 0.6	1,184 ± 32	1.89 ± 0.1%
No. 10	9.5	71	50 ± 0.7	1,022 ± 38	2,04 ± 0.1%

B. BOUNDARY CONDITION

The applied boundary conditions are presented in Figure 2. The applied load combined constant axial load and monotonic-incremental static lateral load. The load is divided into two stages. At the first stage, the column is subjected to 0.1 axial load ratio ($P/A_g f_c'$). The second stage, when the axial load is applied constantly, is the monotonic static lateral displacement. The displacement load is applied through the sides of the upper concrete block. The specimen is supported by roll support on both the right and left sides at the bottom side of the concrete block.

C. MATERIAL PROPERTIES AND CONSTITUTIVE MATERIAL

The concrete compressive strength used in this research was 39 MPa. The confined concrete constitutive plasticity

$$f(\rho,\varepsilon,\theta) = \left(\frac{\sqrt{1.5}\rho}{f_c' qh(k)}\right)^2 + m\alpha\left[\frac{\rho}{\sqrt{6}f_c' qh(k)} r(\theta,e) + \frac{\xi}{\sqrt{3}f_c' qh(k)}\right] - q_s(k) \leq 0$$

. where f'_c is the uniaxial compressive strength of the concrete; k is the hardening parameter; $q_h(k)$ is a hardening function; $q_s(k)$ is the softening function; $r(\theta,e)$ is an ellipse function; e is the eccentricity; m is the friction parameter; a is the friction parameter axis; and (ρ,ξ,θ) are cylindrical coordinates. The parameter that characterize the constitutive model based above are summarized in Table 2. The value of parameters is used as input in 3D-NLFEA finite elemen software can be seen in Table 2.

Table 2. Constitutive Parameters of Concrete Model

Parameter	Value
Compressive Strength (MPa)	39.50
Uniaxial Tensile Strength (MPa)	3.07
Poisson Ratio	0.20
Density (kg/m3)	2400
Internal Length Scale (mm)	50.00
Elastic Modulus (MPa)	27816
Freeze Fracture Direction	1

The stress-strain of steel rebar is modeled with bilinear relationship or perfectly elastic-plastic. The stress of steel with this bilinear model refers to a material model where two lines describe material behaviour. The first line represents the initial elastic phase, with the modulus of elasticity of steel, Es, as its value. The second line represents the plastic phase, characterized by material hardening, with its gradient being the strain-hardening modulus, Esh. In the context of perfect plasticity, when Esh = 0, the strain limit εL indicates the limited ductility of the steel, as shown in Figure 2.

One model of the GFRP stress-strain curve is an asymmetrical stress-strain behavior, as shown in Figure 3. According to research by [11], GFRP reinforcement has a threaded geometry that leads to a reduction in its tensile strength. The compressive strength of GFRP reinforcement decreases to 25% of its ultimate tensile capacity.

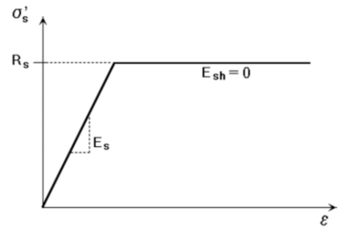

Figure 2. Stress – strain relationship of steel rebar

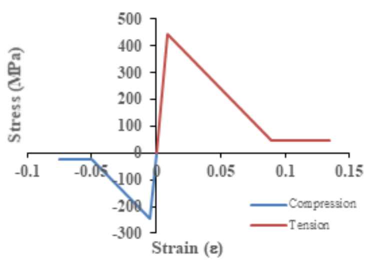

Figure 3. Stress – strain relationship of GRFP rebar

D. FINITE ELEMENT

The use of three-dimensional finite element methods is widely applied due to their advantages in efficiency, flexibility, and cost-effectiveness under certain conditions [11]. The numerical simulation uses 3DNLFEA program. This program series utilizes SALOME 9.3.0 as the pre-processor and Paraview 5.9.1 as the post-processor tool. The 3D-NLFEA package uses hexahedral elements to model concrete elements, adopting Bar element technology (selective integration). In their research, [11] the steel plates were assumed to be modelled using the Von Mises criterion with a perfectly elastic-plastic model. The steel reinforcement was also modeled as perfectly elastic-plastic. Material properties for the GFRP reinforcement used a non-symmetric stress-strain curve for compression and tension.

E. BOUNDARY CONDITION

Boundary conditions are used to simulate the model conditions during the experiment. The boundary conditions on the model will involve defining parts of the element for the application of loads and supports, with using the SALOME program. In this study, the load application includes a constant axial load of 0.1 Ag fc' and lateral load, it shown in Figure 4. In the 3DNLFEA program, the axial load is evenly distributed on the surface of the steel plate and divided into 50 steps.

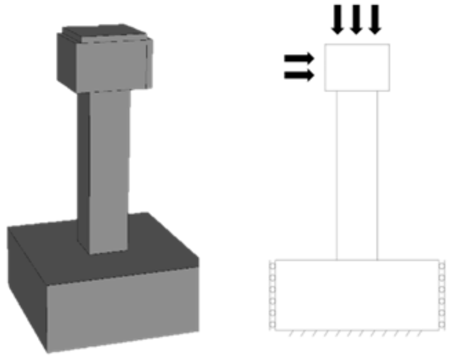

Figure 4. Specimen 3D Model and Applied Boundary Condition

RESULTS AND DISCUSSIONS

The finite element analysis of G-1.3-10-100 model provides the load-displacement relationship, the strain-displacement relationship of the longitudinal bar and the strain-displacement relationship of the transverse bar. All the analysis results are compared with the results from experimental testing.

A. LATERAL LOAD – DRIFT RATIO RESULT

The comparison of the lateral load-drift ratio curves from modeling results and experiments is shown in Figure 4 for an axial load of $P_0 = 0.1\ A_g\ f'_c$. In general, the lateral load-drift ratio curve from 3DNLFEA model exhibits a similar pattern to the experimental result. The curve begins with an elastic phase, followed by the information of cracks until failure, likely due to the idealized assumptions in the model, such as material and the omission of imperfections at the interface. During the elastic phase, the 3DNLFEA model shows more stiffness compared to the experimental results due to the concrete tension strain not reaching the concrete crack strain. This condition persists until the cracking point is reached, but at the peak load, the 3DNLFEA model demonstrates a lower load than that observed in the experiments. At the peak load, the lateral load and drift ratio values from 3DNLFEA results are nearly indistinguishable from the experimental results. This specimen's predicted peak load using 3DNLFEA is 132.602 kN, which occurs at a drift ratio of 6.562%. Meanwhile, from the experimental results, the peak load was obtained 140 kN at drift ratio 6.5%. The post-peak behaviours for both specimen and experimental show similar trend.

For specimens G-1.3-10-100, crushing of concrete along with buckling and compression failure of the longitudinal bars between stirrups occurred simultaneously at 8.5% drift ratio.

B. STRAIN-DRIFT RATIO RESULT

Besides the load-displacement curve, the drift-strain curve illustrates the relationship between drift (the relative lateral displacement between floors or lateral deformation with respect to the height of the structure) and the strain occurring in the structural column elements when subjected to lateral load. In the 3DNLFEA model, this relationship is crucial for understanding how structural elements behave under earthquake loads or other lateral loads that cause lateral deformation in the structure.

In the column elements, drift is calculated as the ratio between the lateral displacement at the top of the column and the total height of the column. Meanwhile, strain is calculated based on the relative change in length of the element due to the applied forces. The relationship between drift and strain provides insights into the level of material.

Figures 5 and 6 show the comparison of drift and strain between numerical and experimental results. The numerical results from the 3DNLFEA simulation showed a similar drift-strain pattern during the early loading stages. Up to a 4% drift ratio, the numerical results indicated that the longitudinal strain produced was close to the experimental results, with minor deviations that were within acceptable limits. However, at higher drift ratios, the numerical results tended to show slightly lower strain compared to the experimental results. This discrepancy could be attributed to the limitations of the numerical model in fully representing the interaction between GFRP reinforcement and the concrete core, as well as the material idealization in the simulation.

Additionally, the numerical results successfully captured the effect of stirrup spacing on the strain distribution in the longitudinal reinforcement. With a stirrup spacing of 100 mm, the numerical model indicated better restraint of the lateral expansion of the concrete compared to specimens with larger stirrup spacing, resulting in lower strain at a given drift. This aligns with the experimental observations, which showed that specimens with smaller stirrup spacing exhibited more controlled lateral deformation.

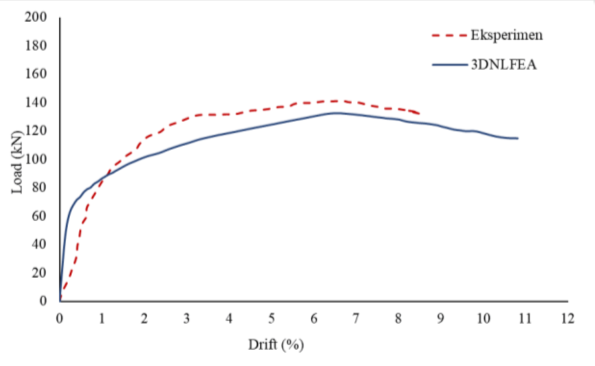

Figure 4. Comparison between model load prediction and experimental result

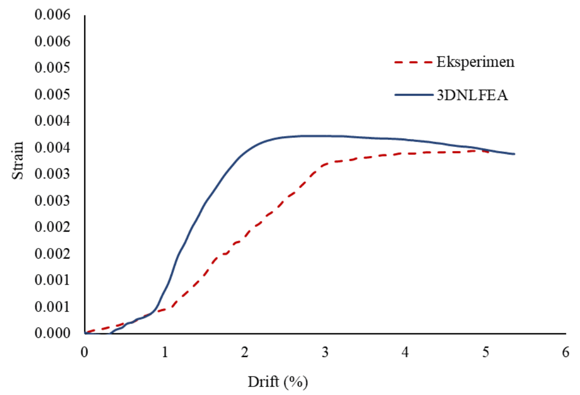

Figure 5. Comparison of maximum strain in longitudinal bar between model and experimental result

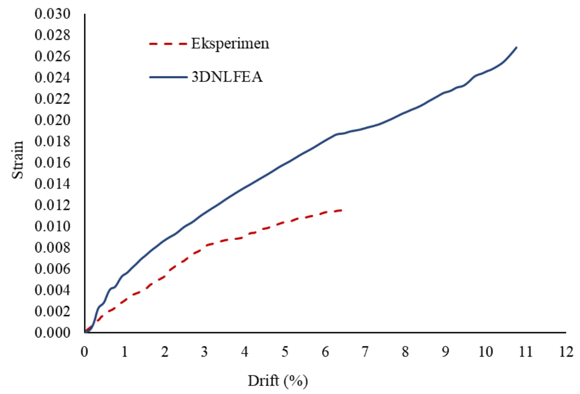

Figure 6. Comparison of maximum strain in transverse bar between model and experimental result

CONCLUSIONS

This research showed a numerical prediction of the behaviour of concrete columns reinforced with GRFP Bar. The specimen is examined under combination of monotonic lateral and axial compression load. The model was performed using 3DNLFEA finite element software. In order to build the specimen, the open-source software of SALOME and Paraview were used as the processor and post-processor, respectively. The analysis result exhibited that the prediction of model behavior corresponds well with the experimental results. The predicted peak load using 3DNLFEA for this specimen is 132.602 kN , which occurs at a drift ratio of 6.562%. Meanwhile, from the experimental results, the peak load was obtained 140 kN at drift ratio 6.5%.

ACKNOWLEDGMENTS

This research was supported by Institut Teknologi Sepuluh Nopember through Penelitian Keilmuan Grant no /PKS/ITS/2024.

REFERENCES

[1] ACI Committee 440, "Guide fo the Design and Construction of Structural Concrete Reinforced with Fiber-Reinforced Polymer (FRP) Bars," American Concrete Institute, America, 2015.

[2] H. Tobbi, A. S. Farghaly and B. Benmokrane, "Concrete Columns Reinforced Longitudinally and Transversally with Glass Fiber-Reinforced Polymer Bars," *ACI STRUCTURAL JOURNAL*, p. 551, 2012.

[3] S. H. T. a. H. N. Rizkalla, "Design recommendations for the use of FRP for reinforcement and strengthening of concrete structures," *Progr. Struct. Eng. Mater*, pp. 16-28, 2003.

[4] M. a. B. B. Theriault, "Effects of FRP Reinforcement Ratio and Concrete Strength on Flexural Behavior of Concrete Beams," *Journal of Composites for Construction*, 1998.

[5] C. C. Choo, I. E. Harik and H. Gesund, "Minimum Reinforcement Ratio for Fiber-Reinforced Polymer Reinforced Concrete Rectangular Columns," *ACI Structural Journal*, 2006.

[6] M. A. A. a. E. El-Salakawy, "Seismic Performance of GFRP-Reinforced Concrete," *J. Compost const.*, 2016.

[7] M. K. Sharbatdar and M. Saatcioglu, "Seismic Design of FRP Reinforced Concrete Structures," *Asian Journal of Applied Sciences*, vol. 2, pp. 211-222, 2009.

[8] A. Tavassoli, J. Liu and S. Sheikh, "Glass Fiber-Reinforced Polymer-Reinforced Circular Columns under Simulated Seismic Loads," *ACI Structural Journal*, vol. 112, pp. 103-114, 2015.

[9] M. A. Ali and El-Salakawy, "Seismic Performance of GFRP-Reinforced Concrete Rectangular Columns," *Journal of Composited for Construction*, 2015.

[10] B. Piscesa, M. M. Attard, A. K. Samani and S. Tangaramvong, "Plasticity Constitutive Model for Stress-Strain Relationship of Confined Concrete," *ACI Structural Journal*, 2017.

[11] A. D. P. B. A. a. P. D. Prasetyo, "3D non-linear finite element analysis of concentrically loaded high strength reinforced concrete column with GFRP bar," *Journal of Civil Engineering*, 2020.

[12] W. P. Wu, "Thermomechanical properties of fiber reinforced plastic (FRP) bars," *Ph.D. dissertation, West Virginia Univ., Morgantown, WV.*, 1990.

[13] B. Piscesa , M. M. Attard, A. K. Samani and S. Tangaramvong, "Plasticity Constitutive Model for Stress-Strain Relationship of Confined Concrete," *ACI Structural Journal,* 2017.

[14] P. Paultre and F. Legeron, "Confinement Reinforcement Design for Reinforced Concrete Columns," *Journal of Structural Engineering* , 2008.

[15] P. Menetrey and K. William, "Triaxial Failure Criterion for Concrete and its Generalization," *ACI Structural Journal,* pp. 311-318, 1995.

[16] P. K. Mallick, "Fiber reinforced composites, materials, manufacturing, and design," *Marcell Dekker,* 1988.

[17] D. L. Logan, A First Course in the Finite Element Method Sixth Edition, USA: Cengage Learning, 2015.

[18] Z. a. S. A. S. Kharal, "Seismic performance of square concrete columns confined with glass fiber-reinforced polymer ties," *J. Compos. Constr.*, 2018.

[19] S. A. Jabbar and B. S. Farid, "Replacement of Steel Rebars by GFRP rebars in the concrete structures," *Karbala International Journal of Modern Science,* pp. 216-227, 2018.

[20] B. K. Elwood, J. Maffei, K. A. Riedere and K. Telleen, "Improving Column Confinement," *Concrete International,* 2009.

[21] M. G. ,. F. A. S. ,. a. B. B. Elshamandy, "Experimental Behavior of Glass Fiber-Reinforced Polymer-Reinforced Concrete Columns under Lateral Cyclic Load," *ACI Structural Journal,* 2018.

[22] V. Cervenka, L. Jendele and J. Cervenka, ATENA Program Documentation Part 1 Theory, Prague: Cervenka Consulting Ltd, 2011.

[23] L. H. B. Bui, B. Stitmannaithum, T. Ueda and ..., "Ductility of Concrete Beams Reinforced with Both Fiber-Reinforced Polymer and Steel Tension Bars," *Journal of Advanced Concrete Technology,* pp. 531-548, 2018.

[24] M. Attard and S. Setunge, "Strees-Strain Relationship of Confined and Unconfined Concrete," *ACI Materials Journal,* pp. 432-442, 1996.

[25] M. K. Anwar , S. A. R. Shah, M. Azab, I. Syah, M. K. S. Chauhan and F. Iqbal, "Structural Performance of GFRP Bars Based High-Strength RC Columns," *MDPI,* 2022.

[26] I. A. T. N. A. A. A. H. Ahmad, "Analisis Pengarus Temperatur terhadap Kuat Tekan Beton," *Jurnal Teknik Sipil,* pp. 63-70, 2009.

[27] C. S. A. "Design and Construction of Building Structures with Fibre-Reinforced Polymers," Canadian Standards Association, Canada, 2012.

[28] A. C. 3. "Building Code Requirments for Structural Concrete (ACI 318-19)," American Concrete Institute, USA, 2019.

[29] M. B. Piscesa, M. Attard, D. Prasetya and A. K. Samani, "Modeling cover spalling behavior in high strength reinforced concrete columns using a plasticity-fracture model," *Engineering Structures,* vol. 196, 2019.